Open Journal of Metal, 2011, 1, 25-33
doi:10.4236/ojmetal.2011.12004 Published Online December 2011 (http://www.SciRP.org/journal/ojmetal)

Preparation and Characteristics of Cu-Al_2O_3 Nanocomposite

F. Shehata[*], **M. Abdelhameed, A. Fathy, M. Elmahdy**
Department of Mechanical Design and Production Engineering,
Faculty of Engineering, Zagazig University, Zagazig, Egypt
E-mail: [*]fshehata@zu.edu.eg

Received October 13, 2011; *revised November* 2, 2011; *accepted November* 20, 2011

Abstract

Thermo-chemical technique was used to synthesize Cu-Al_2O_3 nanocomposite powders. The process was carried out by addition of Cu powder to aqueous solution of aluminum nitrate. Afterwards, a thermal treatment at 850˚C for 1 hr was conducted to get insitu powders of CuO and stable alumina (Al_2O_3). The CuO was reduced in hydrogen atmosphere into copper powder. The nanocomposite powders of both copper and alumina were thoroughly mixed, cold pressed into briquettes and sintered at 850˚C in hydrogen atmosphere. The x-ray diffraction and scanning electron microscope (SEM) with energy dispersive spectrometer (EDS) were used to characterize the structure of the obtained powders. The results showed that alumina nanoparticles (20 nm) and ultra fine copper crystallite (200 nm) were obtained. SEM and EDS showed that the alumina particles were uniformly dispersed within the copper crystallite matrix. The structure also revealed formation of a third phase ($CuAlO_2$) at copper-alumina interface. The hardness and density results showed that the gain in hardness was found to be dependent on the alumina contents rather than on the relative densities. The alumina content up to 12.5% resulted in an increase of 47.9% in hardness and slight decrease (7.6%) in relative densities. The results of compression tests showed considerable increase in compression strength (67%) as alumina content increased up to 12.5%. The compression strength showed further increase in compression strength (24%) as strain rates were increased from 10^{-4} s^{-1} to 10^{-2} s^{-1}. Strain hardening and strain rate parameters "n" and "m" have shown positive values that improved the total strain and they can be used to predict formability of the nanocomposite.

Keywords: Cu-Al_2O_3, Nanocomposite, Thermochemical, Compression, Strain Rate, Strain Hardening

1. Introduction

Copper has been widely used in many industrial applications such as: contact supports, frictional break parts, electrode materials among others [1-5]. Pure copper has relatively low mechanical properties. Alloying of copper with zinc or tin was used to improve the strength of the pure metal. Grain refinement strengthening (or Hall-Petch strengthening) was also used as a method of strengthening copper by changing their average crystallite (grain) size [6]. Recently Metal Matrix Composites (MMCs) and Nano MMC reinforced with ceramic particulates offered significant increase in strength over pure copper and their alloys. The strengths of these composites were found to be proportional to the percentage contents and fineness of the reinforced particles [7]. MMCs with a uniform dispersion of particles smaller than 100 nm size exhibit more outstanding properties over MMCs and are termed Metal Matrix Nano-composites (MMNCs). The MMNCs are also assumed to overcome the shortcoming of MMCs poor ductility. It has been reported that with a small fraction of nano-sized reinforcements, MMNCs could obtain comparable or even far superior mechanical properties than MMCs. The main advantages of MMNCs include excellent mechanical performance, feasible to be used at elevated temperatures, good wear resistance, low creep rate, etc. Preparation and processing of MMNCs have been recently studied, as the processing of such composites is quite a challenge. Though a variety of processing techniques have been explored and studied over the recent years, none have emerged as the optimum-processing route. The major issue that needs to be addressed is the tendency of nano-sized particles to cluster or agglomerate and also the challenge as to how to disperse them uniformly in the matrix structure [8].

Fabrication of the aluminum oxide nanoparticles into copper matrix can be divided into two major methods; ex-situ and in-situ [9]. The ex-situ method is usually cost efficient but the alumina particles tend to agglomerate due to poor wettability between the matrix and reinforcement [10,11]. The in-situ methods can provide fine and uniformly distributed particles but they are usually not cost-effective. Obtaining powders by a thermochemical insitu method, in which the input materials are in the liquid state, is not a new procedure but recently, due to the development of modern materials with cost effective characteristics an intensive interest in thermochemical method for production of ultra fine nano-powders has been emerged [12-14]. According to Jena *et al.* [13] the synthesis of nano-composite powders by a chemical method is possible in two ways. The first method comprises adding of a certain quantity of CuO into a solution of aluminum nitrate. In the second synthesis method, aluminum nitrate and CuO are mixed in appropriate quantities of ammonium hydroxide. In both methods the mixture was annealed at 850˚C and then reduced in a hydrogen atmosphere at 975˚C for 2 h until the final structure was obtained.

Recently Shehata *et al.* [15] used mechanochemical method with two different routes to synthesize the Cu-Al_2O_3 nanocomposite powders. First, route-A was carried out by addition of Cu to aqueous solution of aluminum nitrate, and second, route-B was also carried out by addition of Cu to aqueous solution of aluminum nitrate and ammonium hydroxide. In both routes, the mixtures were heated in air, reduced in hydrogen atmosphere and milled mechanically to get ultra fine powder oxides of CuO and Al_2O_3.

The objective of the present work is intended to produce of Cu-Al_2O_3 nanocomposites with various alumina contents using cost effective method using insitu thermochemical technique without any milling. The technique comprises adding of a certain quantity of cheap micro copper powder into a solution of aluminum nitrate as starting materials. The structure characteristics and physical and mechanical behaviour of the obtained nanocomposite and monolithic copper were examined, presented and analysed.

2. Experimental Work

The desired amount of copper powder and aluminum nitrate $Al(NO_3)_3$ were thoroughly mixed and used as starting solution to synthesize nanocomposite of Cu-Al_2O_3 powders. The alumina loadings were adjusted to be 2.5, 7.5 and 12.5 wt% of the final composites, so that we can investigate the impact of alumina contents on the mechanical and physical properties of the obtained composites.

The solution of copper and aluminum nitrate was spray dried at 180˚C to produce the precursor powder. The precursor powder was heated to 850˚C in an open air for one hour; thereby copper oxide (CuO) and the thermodynamically stable phase (α-Al_2O_3) were formed according to following Equation:

$$\mathrm{Cu}+\mathrm{Al}\left(\mathrm{NO}_3\right)_3 \rightarrow \left(\mathrm{CuO}+\mathrm{Al}_2\mathrm{O}_3\right)+6\mathrm{NO}_2\uparrow+\mathrm{O}_2\uparrow \quad (1)$$

The obtained powders of CuO and Al_2O_3 were thermally treated in a hydrogen atmosphere at a temperature of 500˚C for 30 minutes, whereby the copper oxide was reduced and transformed into elementary copper and the Al_2O_3 remained unchanged.

Using powder metallurgy technique, the thermally treated powders were pressed from the top side in a cylindrical mould at 600 MPa and sintered at 850˚C for 120 minutes in a hydrogen atmosphere. Previous publications by the authors give a detailed description of the procedures [15].

X-ray diffractmeter with Cu Ka radiation was used to assess the formation of phase's transformation and to measure the crystallite size of powders using the Scherer's formula [16]. Composite powder was examined using scanning electron microscopy (SEM) with energy dispersive spectrometer (EDS).

Relative densities were calculated as the ratio of the experimental to the theoretical densities of samples. Experimental densities were determined by the Archimedes method and the theoretical densities were calculated from the simple rule of mixtures, taking the fully dense values for copper as 8.94 g/cm^3 and alumina as 3.95 g/cm^3. Hardness measurements of the composite samples have been measured using Brinell hardness testing machine. Tests were conducted using a steel ball indenter of 2.5 mm diameter and load of 62.5 kg force. At least five measurements of hardness and density were performed on each sample.

The compression tests were carried out using a hydraulic testing machine. The stress versus strain curves were obtained over an initial strain rates of 10^{-4} s^{-1}, 10^{-3} s^{-1} and 10^{-2} s^{-1}. Cylindrical specimens with height 12 mm and diameter 12 mm were used in compliance with ASTM standards (E9-89a) for measuring the compressive response of the matrix and composite materials [17]. Special graphite-based grease is placed between the tested specimen and the platen of the compression machine to minimize the friction. The percentage reduction was performed up to 50% reduction in height; some specimens were fractured before reaching 50% height reduction.

3. Results and Discussions

3.1. Structural Evolutions

Figure 1 shows X-ray diffraction (XRD) patterns of nanocomposite (Cu-12.5% Al_2O_3) powders after thermal treating and before CuO reduction. The XRD pattern shows three crystalline peaks that were identified as CuO, Al_2O_3 and $CuAlO_2$. The particle size of alumina, (Al_2O_3) was calculated from X-ray line broadening using Scherer's formula ($D = 0.9\lambda/B\cos\theta$), where, D is the crystallite size, λ is the wavelength of the radiation, θ is the Bragg's angle and B is the full width at half maximum [16]. The size of alumina nanoparticles showed a value of 20 nm whilst size of copper crystallites were 200 nm. The third peak corresponds to a third phase of $CuAlO_2$. The formation of this phase is thermodynamicaclly possible on Cu-Al contact surfaces. The formed third phase influences the nature of the interface bonds and dislocation motions. It greatly improves both the mechanical and electrical properties of the sintered systems [23].

The CuO is reduced to Cu via an intermediate phase of Cu_2O rather than undergoing a direct reduction to elemental copper [18]. However, the nanoparticles phase of Al_2O_3 remained in the unchanged form after hydrogen reduction process. The alumina particles are uniformly dispersed within the copper matrix. X-ray diffraction of powder after the reduction by hydrogen showed presence of two peaks that correspond to the elementary copper and Al_2O_3 nano particles as shown in **Figure 2**. In accordance with the experimental set-up, only the peaks which correspond to elementary copper and Al_2O_3 particles

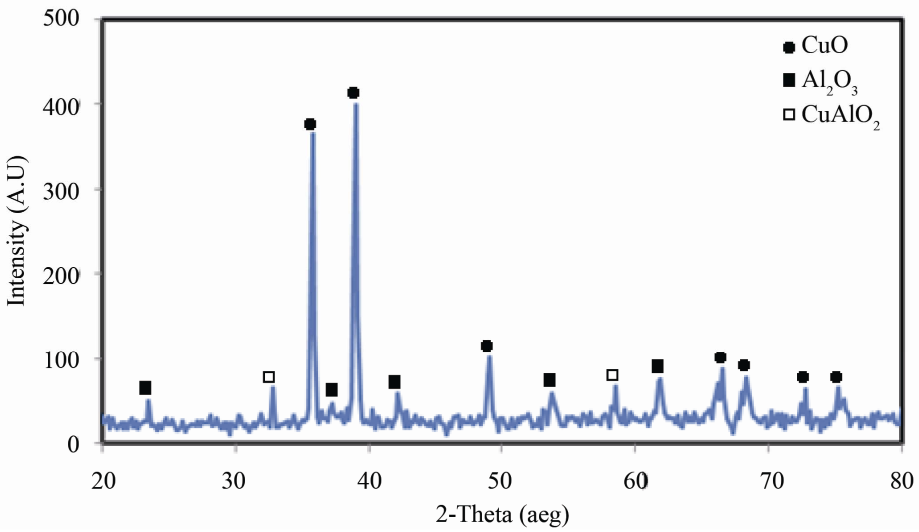

Figure 1. X-ray diffraction analyses of a Cu-Al_2O_3 samples containing 12.5% alumina showing CuO, Al_2O_3 and $CuAlO_2$ peaks.

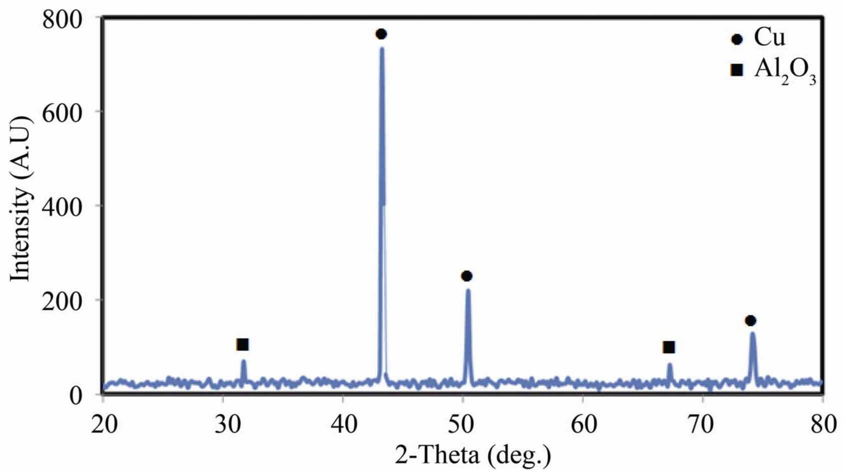

Figure 2. X-ray diffraction analyses of a Cu-Al_2O_3 samples containing 12.5% alumina powder after reduction.

were registered in the structure. The intensity of the Al_2O_3 peaks showed lower intensity values than copper. The alumina intensity values are not up to the proportion of the 12.5% alumina. The reason may be attributed to the facts that alumina particles are extremely small that they are embedded in the copper matrix.

The obtained Cu-Al_2O_3 powders were characterized by Scanning Electronic Microscopy (SEM) and with an energy spectrum analyzer (EDS) as presented in **Figure 3**. Nano particle sizes are noticeable with sizes less than 100 nm. The presences of agglomeration as well as nodular individual particles are seen in the structure. Most particles have rough surface morphology. The particle sizes seemed to be slightly increased as contents of alumina are increased from 2.5% to 12.5 %. The alumina particulate dispersion could inhibit the movement of the grain boundaries and consequently the grain growth. The agglomeration of particles as a result of sintering process resulted in larger particle sizes as seen by SEM than that obtained from XRD.

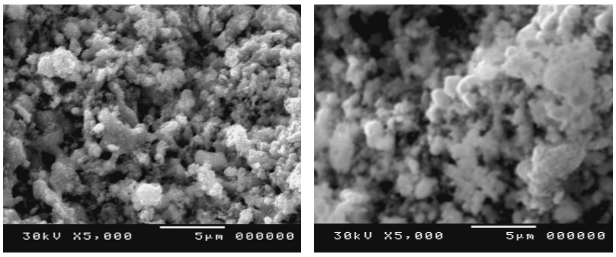

Figure 3. SEM and EDS analysis micrograph of the Cu-Al_2O_3 nanocomposite powders.

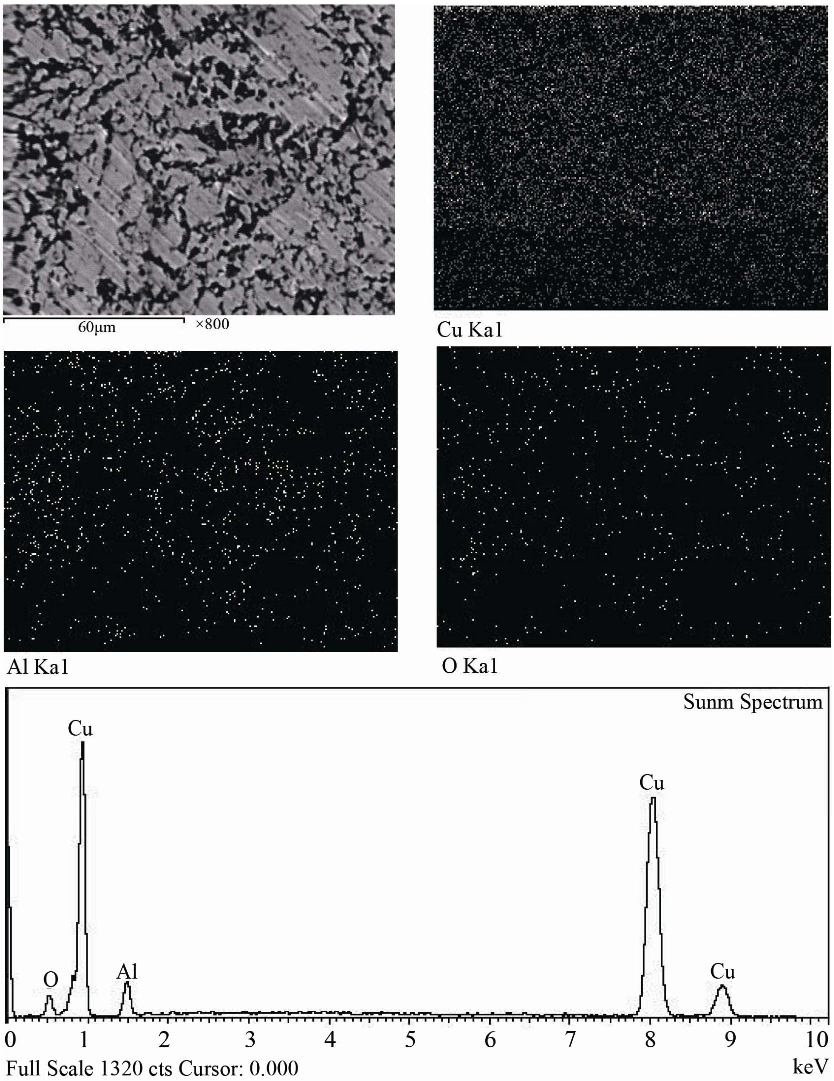

Figure 4. SEM image and EDS surface scanning of Cu-12.5 % Al_2O_3 composite, showing distribution of the Cu (Top right), Al (middle left) and oxygen (middle right) .

Figure 4 shows images of SEM and Electron Dispersive

Spectrum (EDS) of sintered Cu-12.5% Al_2O_3 nanocomposite. The SEM image indicates fairly homogeneous distribution of alumina in Cu matrix. EDS image scan indicates that uniform distribution of Cu, Al and O elements all over surface. The level of copper is much higher than that of aluminum and oxygen. The EDS results revealed locations with a relatively high concentration of Al and O elements. These locations were thought as being "Al_2O_3-rich" which may represent the presence of a third phase of $CuAlO_2$ (spinel) at interface between alumina particles and copper crystallites matrix. The spinel phase forms a strong bond at the interfaces.It was found that the Al and O are not limited to specific regions, but they are dispersed and overlapping throughout the entire microstructure surface. It can also be noticed that a concentration gradient instead of an abrupt change of elements at the metal/ceramic interface. The particle is surrounded by another region with decreasing composition of Al and O and increasing amount of Cu towards the Cu matrix. This gradual change in concentration indicates forming of a third phase compound such as $CuAlO_2$ or $CuAlO_4$ in the material. Furthermore, the elemental copper covers almost the entire surface of the as shown in top right of the figure. The aluminum and oxygen elements are present in fewer values in the structure.

In order to further identify the Al_2O_3 particles within the Cu-Al_2O_3 nanocomposite powder before sintering. The powder was flushed with 10% nitric acid to selectively dissolve the copper and keep the alumina (Al_2O_3) nanoparticles. Alumina nanoparticles were then extracted by filtering through 0.5 micron mesh. After the final filtration, the sample was dried in air at room temperature for 24 h. **Figure 5** shows SEM bright field image of the extracted Al_2O_3 nanoparticles. SEM observations showed that the particles of Al_2O_3 in the composite powder produced have sizes ranged from 20 to 60 nm. Most particles showed regular and nearly nodular shape appearance.

3.2. Physical and Mechanical Properties

Nanocomposite materials are expected to have special physical and mechanical properties particularly in the case of the Cu-Al_2O_3 nanocomposites. Alumina particles can be uniformly dispersed in a Cu matrix, providing unique characteristics, such as high degree of strength without great loss in plastic deformation. The particulate dispersion may inhibit the movement of both dislocations and grain boundaries. In this regard, Al_2O_3 has been used as a ceramic dispersion phase in many cases because of its low price and its excellent chemical stability. **Table 1** shows the relative density and hardness of nanocomposites at various alumina contents.

The gain in hardness was found to be dependent on the alumina contents rather than on the relative densities. Slight decrease in relative densities was noticed as alumina percentage was increased. This is an indication of the presence of slight voids in nanocrystalline metals that would undoubtedly lead to weaker mechanical properties. However, the hardness values showed an increase of 47.9% as alumina contents are increased up to 12.5% Al_2O_3. Whilst relative densities values showed a decrease of only 7.6% as alumina contents were increased by same amounts. The gain in hardness may be attributed to the dispersion of alumina nanoparticles and the strong bond at the copper-alumina interfaces resulted from presence of the third phase ($CuAlO_2$).

There are many factors which influence the composites mechanical properties such as hardness, compression strength, speed of loading or strain rate etc. In this regard compression strength at various strain rates have been carried out to assess the toughness and formability of Cu-Al_2O_3 nanocomposite. **Figure 6** shows typical compressive stress-strain curves for nanocomposites of various

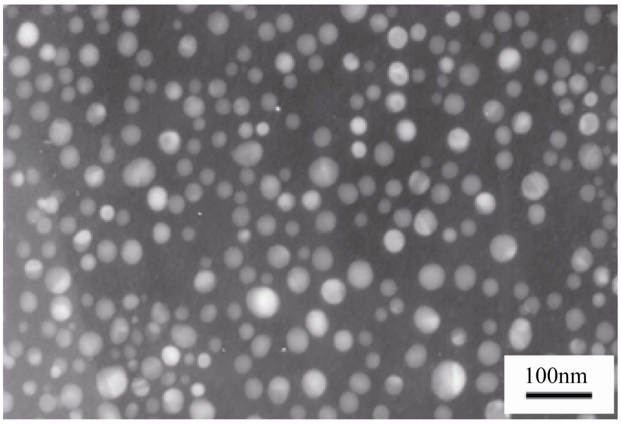

Figure 5. SEM bright field image of the extracted Al_2O_3 nanoparticles.

Table 1. Relative density and hardness of Cu-Al_2O_3 samples.

Composites	Relative Density %	Brinell hardness (BHN)
Cu	95.11	43.70
Cu-2.5wt.% Al_2O_3	92.53	59.83
Cu-7.5wt.% Al_2O_3	89.99	67.90
Cu-12.5wt. % Al_2O_3	87.86	79.40

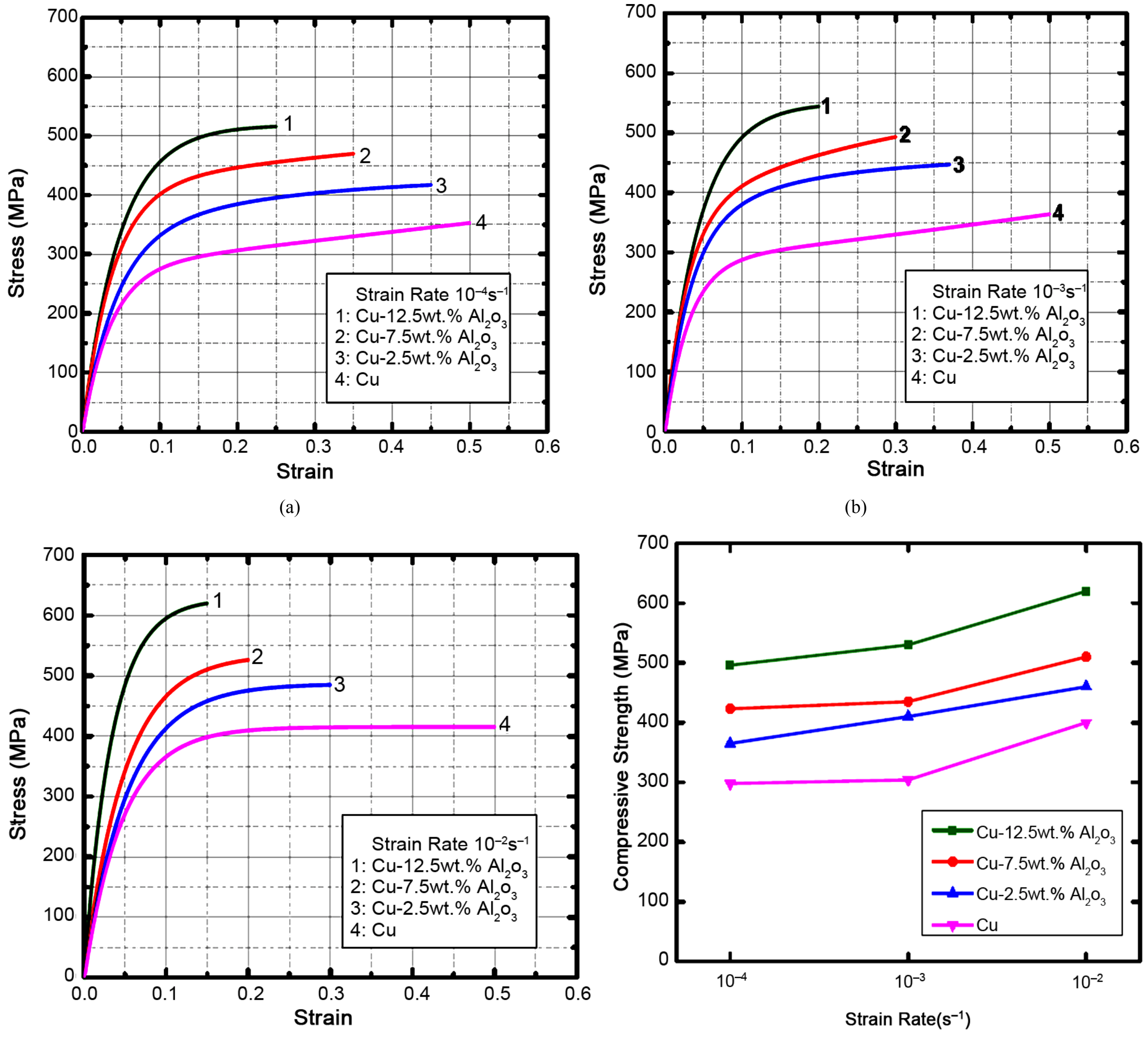

(a) (b)

(c) (d)

Figure 6. Compression stress-strain curves of Cu-Al$_2$O$_3$ nanocomposites. (a) $\varepsilon^{\cdot} = 10^{-4}\ \text{s}^{-1}$ (b) $\varepsilon^{\cdot} = 10^{-3}\ \text{s}^{-1}$ (c) $\varepsilon^{\cdot} = 10^{-2}\ \text{s}^{-1}$ and (d) σ vs. $\varepsilon^{\cdot}$.

alumina contents. The tests were carried out at initial strain rates of $10^{-4}\ \text{s}^{-1}$, $10^{-3}\ \text{s}^{-1}$ and $10^{-2}\ \text{s}^{-1}$ at room temperature. **Figure 6(d)** summarizes the effect of strain rates on compressive strengths at a specific strain of 0.15. Figures illustrate that the compressive strength of the Cu-Al$_2$O$_3$ nanocomposite is much higher than that of monolithic copper at all tested strain rates. A significant increase in compressive strengths can be achieved by increasing the alumina contents up to 12.5%. At fixed strain of 0.15, the compressive strength increased from 300 to 500 MPa as alumina is increased to 12.5%. *i.e.* an increase of 67 %. Further increase in the strength could be achieved by increasing strain rate. Compressive strength is increased from 500 to 620 MPa as strain rate is increased from $10^{-4}\ \text{s}^{-1}$ (**Figure 6(a)**) to strain rate of $10^{-2}\ \text{s}^{-1}$ (**Figure 6(c)**) *i.e.* an increase of 24%. However increasing alumina contents and increasing strain rates generally resulted in ductility decrease 40% - 55%.

An attempt was made to quantify the possible strengthening effects of the nanocomposite copper materials with Al$_2$O$_3$ dispersoids. Two strengthening mechanisms were proposed for high hardness and compression strength of the materials, *i.e.*, grain size and dispersion hardening effects [19]. The main strengthening of metallic materials is based on preventing dislocation motion and propagation. However, there is a limit to this mode of strengthening in nanocomposite. Grain sizes can range from about 100 μm to 1 μm in traditional materials whilst in nanocomposite materials the grains are less than 100 nm. At grain size of about 10 nm only one or two dislocations can fit inside a grain [20]. This small numbers of dislocations inside the grains may prohibit the dislocation pile-up and grain boundary diffusion. The lattice would resolve the applied stress then by grain boundary sliding [21], resulting in a decrease in the material strength and increase in ductility.

However, experiments on many nanocrystalline materials demonstrated that if the grains reached a small enough size, the compression strength would either remain constant or decrease with decreasing grains size. This phenomenon has been termed as the reverse or inverse Hall-Petch Relation [22].

Furthermore, the alumina nanometric particulates cause dispersion hardening effects that impede dislocation motion, increasing the compressive strength of the material. In addition to the formation of the third phase that causes great reinforcement at copper-alumina interface. It has been concluded that the binding mechanisms on copper-third phase or alumina-third phase interfaces are considerably stronger than copper-alumina interfaces [23]. Therefore, the presence of uniform distribution of fine alumina particles and formation of the third phase are considered as the main reinforcing parameters causing a considerable increase in compression strengths of the Cu-Al_2O_3 nanocomposite.

The strain hardening exponent (n) was calculated from the true stress-strain curves for a strain range between 0.10 and 0.15 using the following equation:

$$n = \frac{\ln(\sigma_1/\sigma_2)}{\ln(\varepsilon_1/\varepsilon_2)} \tag{2}$$

Where σ_1 and σ_2 are stresses at the corresponding strain ε_1 and ε_2.

Figure 7 shows the effect of strain rate on the strain hardening exponent (n) of nanocomposite materials and monolithic copper. The strain hardening exponent "n" seemed to be generally increased as strain rate is increased. The values of "n" have increased as the strain rates were increased up to 10^{-3} s^{-1}. At higher strain rate, the 'n' values have slightly decreased with increase of the strain rate from 10^{-3} s^{-1} to 10^{-2} s^{-1}. The maximum "n" was found at strain rate of 10^{-3} s^{-1}. Values of "n" for nanocomposite were found to be higher than that of the monolithic copper. Higher n values generally lead to higher compressive strength. The increase of n values may be attributed to the dynamic strain ageing effects that enhance the strain hardening and reduce the dynamic recovery [19]. Dynamic strain aging is a phenomenon in which the nanoparticles of alumina may diffuse around dislocations and inhibit dislocation motion.

The reason for decrease in n-value at the higher strain rate (10^{-2} s^{-1}) is probably due to thermal softening. At higher strain rates, the temperatures are increased than the desired specific temperature which leads to thermal softening [5]. At higher temperatures, the dislocation loops can multiply and move from plane to plane by cross-slip, the processes that lead to a recovery of mechanical properties producing a wide plastic deformation.

On the other hand, the strain rate hardening exponents (m) were calculated from the true stress-strain curves for a strain range between 0.10 and 0.15. The value of "m" is calculated by comparing the stress-strain curves of monolithic copper and nanocomposite materials at two different strain rates $\varepsilon_1^{\bullet}$ and $\varepsilon_2^{\bullet}$. The simplest method is reflected in the relationship between the flow stress (σ) and the strain rate ($\varepsilon^{\bullet}$) using the following Equation:

$$m = \frac{\ln(\sigma_1/\sigma_2)}{\ln(\varepsilon_1^{\bullet}/\varepsilon_2^{\bullet})} \tag{3}$$

where σ_1 and σ_2 are stresses at the corresponding strain rates $\varepsilon_1^{\bullet}$ and $\varepsilon_2^{\bullet}$.

Figure 8 shows the effect of strain on the strain rate sensitivity exponent (m) of nanocomposite and monolithic copper. The m-values were calculated between strain rates of 10^{-4} and 10^{-3} s^{-1} (**Figure 6(a)**) and between 10^{-4} and 10^{-2} s^{-1} (**Figure 6(b)**). The values of m have shown to be decreased as the strain is increased from 0.10 to 0.20 in both figures. The maximum 'm' values are observed for monolithic copper and for nanocomposites of the smallest alumina contents. Moreover, the wider strain rates at which m were calculated (10^{-4} s^{-1} and10^{-2} s^{-1}) showed higher m-values compared to the.

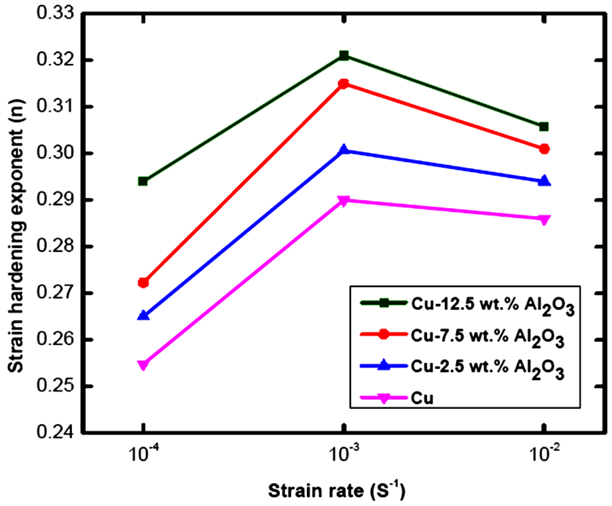

Figure 7. Effect of strain rate on strain hardening exponent (n).

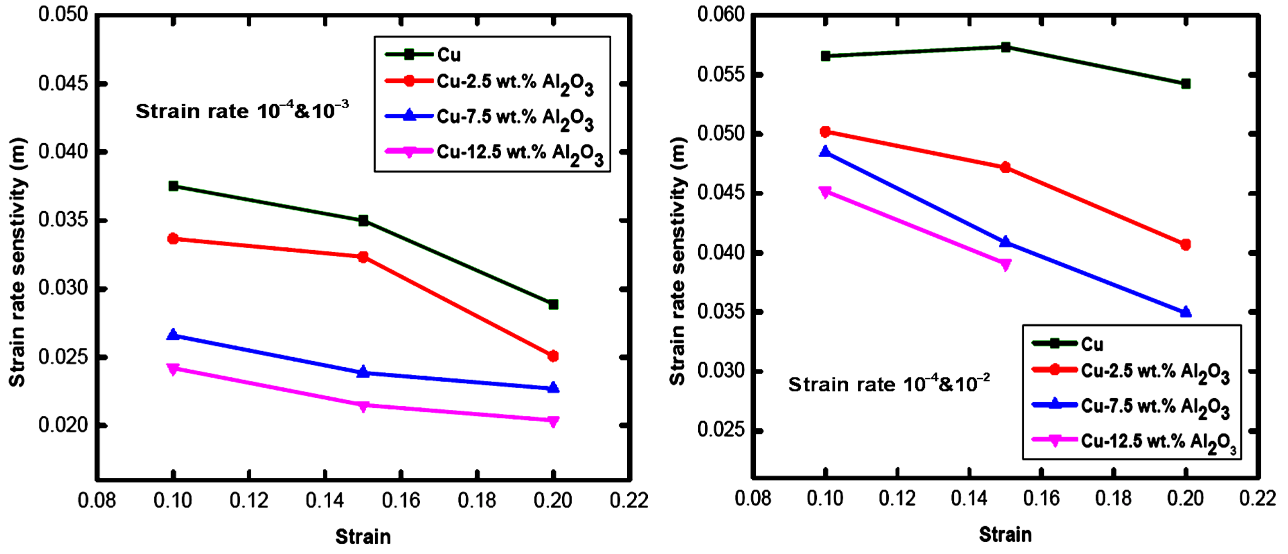

(a) (b)

Figure 8. Strain rate exponent "m" against strain of Cu-Al$_2$O$_3$ nanocomposites Strain rates between 10^{-4} and 10^{-3} s^{-1} (b) Strain rates between 10^{-4} and 10^{-2} s^{-1}.

narrower strain rates (10^{-4} and 10^{-3} s^{-1}). In both strain rate combinations, m-values of the nanocomposite showed smaller values than that of the corresponding monolithic copper

The positive increase in "n" and "m" values would result in improvement of both uniform and post uniform strains to failure and therefore improves the formability of the material. The easy obtained parameters "n" and "m" can be used to predict the formability of the nanocomposite materials in nearly the same way as in traditional materials.

4. Conclusions

The following conclusions can be made from the present study:

1) Monolithic Cu and Cu-Al$_2$O$_3$ nanocomposites powders can be successfully synthesized using the thermochemical technique followed by pressing and sintering.

2) Thermochemical process gave nanoparticles of alumina of 20 nm size that are uniformly dispersed within Cu-matrix. Significant grain refinement of copper was formed.

3) Formation of pronounced third phase (CuAlO$_2$) revealed at copper-alumina interface that causes strong bond at the interface.

4) Increasing alumina up to 12.5% copper led to a significant improvement in hardness of 47.9%, and an increase of compressive strength by 67 %.

5) Increasing strain rate from 10^{-4} s^{-1} to 10^{-2} s^{-1} further increased compressive strengths by 24%.

6) Increasing both alumina contents and strain rates resulted in ductility decrease by 40% - 55%.

7) The positive values of "n" and "m" at room temperature increase the total strain to fracture and therefore increase the formability of the composite. Parameters "n" and "m" can be used to predict the formability of the nanocomposite materials.

5. References

[1] D. W. Lee and B. K. Kim, "Nanocomposite Powders for New Contact Materials Based on Copper And Alumina," *Materials Letters*, Vol. 58, No. 3-4, 2004, pp. 378-383. doi:10.1016/S0167-577X(03)00505-6

[2] G. M. Kalinin, S. A. Fabritsiev and B. N, "Specification of Properties and Design Allowable for Copper Alloys Used in HHF Components of ITER," *Journal of Nuclear Materials*, Vol. 307-311, 2002, pp. 668-672.

[3] R. H. Liu, K. X. Song, S. G. Jia, X. F. Xu, J. X. Gao, X. H. Guo, "Morphology and Frictional Characteristics Under Electrical Currents of Al$_2$O$_3$/Cu Composites Prepared by Internal Oxidation," *Chinese Journal Aeronautic*, Vol. 21, No. 3, 2008, pp. 281-288. doi:10.1016/S1000-9361(08)60037-0

[4] H. Nasiri, J. Vahdati Khaki and S. M. Zebarjad, "One-Step Fabrication of Cu-Al$_2$O$_3$ Nanocomposite via Solution Combustion Synthesis Route," *Journal of Alloys and Compounds*, Vol. 509, No. 17, 2011, pp. 5305-5308. doi:10.1016/j.jallcom.2011.01.185

[5] J. R. Groza and J. C. Gibeling, "Principles of Particle Selection for Dispersion-Strengthened Copper," *Materials Science and Engineering A*, Vol. 171, No. 1-2, 1993, pp. pp. 115-125. doi:10.1016/0921-5093(93)90398-X

[6] J. R. Weertman, "Structure and Mechanical Behavior of Bulk Nanocrystalline Materials," *MRS Bulletin*, Vol. 24,

No. 2, 1999, pp. 44-50.

[7] G. B. Veeresh Kumar, C. S. P. Rao and N. Selvaraj, "Mechanical and Tribological Behavior of Particulate Rein- forced Aluminum Metal Matrix Composites—A Review," *Journal of Minerals & Materials Characterization & En- gineering*, Vol. 10, No.1, 2011, pp. 59-91.

[8] E. T. Thostenson, C. Li and T. W. Chou, "Review: Nanocomposites in Context," *Composites Science and Technology*, Vol. 65, No. 3-4, 2005, pp. 491-516. doi:10.1016/j.compscitech.2004.11.003

[9] F. He, Q. Han and M. J. Jackson, "Nanoparticulate Reinforced Metal Matrix Nanocomposites—A Review," *International Journal of Nanoparticles*, Vol. 1, No. 4, 2008, pp. 301-309.

[10] R. Ashtana, "Solidification Processing of Reinforced Metals," *Transaction Technical Publications*, Vol. 151-152, 1997.

[11] A. Evans, C. San Marchi amd A. Mortensen, "Metal Matrix Composites in Industry: An Introduction and a Survey," Springer, Berlin, 2003. doi:10.1007/978-1-4615-0405-4

[12] M. Korac, Z. Kamberovic, M. Tasic and M. Gavrillovski, "Nanocomposite Powders for New Contact Materials Based on Copper and Alumina," *Chemical Industry & Chemical Engineering Quarterly*, Vol. 14, No. 4, 2008, pp. 215-218. doi:10.2298/CICEQ0804215K

[13] P. K. Jena, E. A. Brocchi and M. S. Motta, "Identification of a Third Phase in Cu-Al_2O_3 Nanocomposites Prepared by Chemical Routes," *Material Science Engineering A*, Vol. 371, No. 1-2, 2004, pp. 72-78.

[14] M. Korać, Z. Anđić, M. Tasić and Z. Kamberović, "Sintering of Cu-Al_2O_3 Nanocomposite Powders Produced by a Thermochemical Route," *Journal of Serbian Chemistry Society*, Vol. 72, No. 11, 2007, pp. 1115-1125.

[15] F. Shehata, A. Fathy, M. Abdelhameed and S. Moustafa, "Preparation and Properties of Al_2O_3 Nanoparticle Reinforced Copper Matrix Composites by *In Situ* Processing," *Materials & Design*, Vol. 30, No. 7, 2009, pp. 2756-2762. doi:10.1016/j.matdes.2008.10.005

[16] B. D. Cullity, "Elements of X-Ray Diffraction," 2nd Edition, Addison-Wesley, Boston, 1978, p. 102.

[17] D. J. Towle and C. M. Friend, "Comparison of Compressive and Tensile Properties of Mg Based MMCs," *Materials Science Technology*, Vol. 9, No. 1, 1993, pp. 35-41.

[18] J. Pike, S.W. Chan, F. Zhang, *et al*., "Formation of Stable Cu_2O from Reduction of CuO Nanoparticles," *Applied Catalysis A*: *General*, Vol. 303, No. 2, 2006, pp. 273-277. doi:10.1016/j.apcata.2006.02.008

[19] S. J. Hwang, "Compressive Yield Strength of the Nanocrystalline Cu with Al_2O_3 Dispersoid," *Journal of Alloys and Compounds*, Vol. 509, No. 5, 2011, pp. 2355-2359. doi:10.1016/j.jallcom.2010.11.017

[20] C. A. Schuh and T. G. Nieh, "Hardness and Abrasion Resistance of Nanocrystalline Nickel Alloys near the Hall-Petch Breakdown Regime," *Proceedings of Symposium I*, *Nanomaterials for Structural Applications*, Boston, 2-6 December 2003, pp. 27-32.

[21] J. Schiotz, F. D. Di Tolla and K. W. Jacobsen, "Softening of Nanocrystalline Metals at Very Small Grains," *Nature*, Vol. 391, No. , 1998, pp. 561-563. doi:10.1016/j.jallcom.2010.11.017

[22] H. Conrad and J. Narayan "On the Grain Size Softening in Nanocrystalline Materials," *Script Material*, Vol. 42, No. 11, 2000, pp. 1025-1030. doi:10.1016/S1359-6462(00)00320-1

[23] M. Korac, Z. Kamberovic, Z. Andic, M. Filippovic and M. Tasic, "Sintered Materials Based on Alumina and Copper Powders Synthesized by a Novel Method," *Science of sintering*, Vol. 42, No. 1, 2010, pp. 81-90. doi:10.1016/S1359-6462(00)00320-1